Supporting Information for

Tuning of spin-crossover behavior in two cyano-bridged mixed-valence $Fe^{III}_2Fe^{II}$ trinuclear complexes based on Tp^R ligand

Arshia Sulaiman,[a] Yi-Zhan Jiang,[a] Mohammad Khurram Javed,[a] Shu-Qi Wu,[b] Zhao-Yang Li[a] and Xian-He Bu[a, c]*

[a]*School of Materials Science and Engineering, Nankai University, 38 Tongyan Road, Tianjin 300350, China*

[b]*Institute for Materials Chemistry and Engineering & IRCCS, Kyushu University, 744 Motooka, Nishi-ku, Fukuoka 819-0395, Japan*

[c]*College of Chemistry, Nankai University, 94 Weijin Road, Tianjin 300071, China*

Experimental Section

1. Synthesis

All reagents and solvents were purchased from commercial sources and used for the syntheses without further purification. The ligand TPMA was prepared according to methods in the literature[1]. The synthesis of intermediate compounds $[NEt_4][Fe^{III}(Tp^R)(CN)_3]$ were carried out according to a previously reported procedure with slight modifications.[2]

Synthesis of $\{[Fe^{II}(TPMA)][Fe^{III}(Tp^*)(CN)_3]_2\}\cdot MeOH\cdot 2H_2O$

A 2.5 ml H_2O/MeOH (1:4) solution containing $Fe(ClO_4)_2\cdot 6H_2O$ (0.0025 g, 0.01 mmol) and TPMA (0.0029 g, 0.01 mmol) was placed at the bottom of the test tube and a 2 ml methanol solution containing $[NEt_4][Fe^{III}(Tp^*)(CN)_3]$ (0.0084 g, 0.015 mmol) were layered on the solution. One week later, the crystals of the target compound were obtained in the middle of the test tube with a 68% yield. Elemental analysis (%) of $C_{55}H_{70}B_2Fe_3N_{22}O_3$(M = 1276.47): C, 51.75; H, 5.53; N, 24.14; Experimental values：C, 52.01; H, 5.33; N, 23.91. IR (KBr tablet, cm^{-1}): 3409 (br), 2926 (w), 2516 (w), 2360 (w), 2118 (s), 1637 (m), 1608 (m), 1544(s), 1481(w),1448 (vs), 1416 (vs), 1383 (s), 1370 (s), 1304 (s), 1203 (vs), 1156 (w), 1060 (vs), 983 (w), 883 (w), 867 (w), 815 (w), 782 (w), 736 (s), 691 (m), 644 (m), 503 (w).

Synthesis of $\{[Fe^{II}(TPMA)][Fe^{III}(Tp)(CN)_3]_2\}\cdot H_2O$

Complex **2** was synthesized in the same way as complex **1**. $[NEt_4][Fe^{III}(Tp)(CN)_3]$ (0.008 g, 0.015 mmol) was used instead of $[NEt_4][Fe^{III}(Tp^*)(CN)_3]$. The crystals of the target compound were obtained in the middle of the test tube with a 71% yield. Elemental analysis (%) of $C_{42}H_{38}B_2Fe_3N_{22}$ (M = 1040.1): C, 48.13; H, 4.42; N, 29.4; Experimental values: C, 48.57; H, 4.33; N, 29.15. IR (KBr tablet, cm^{-1}): 3455 (br), 3116 (w), 2922 (w), 2513 (s), 2345 (s), 2128 (vs), 1602 (m), 1570 (w), 1499 (m), 1479 (w), 1440 (w), 1405 (s), 1312 (vs), 1212 (vs), 1154 (w), 1113 (s), 1048 (vs), 1072 (w), 1017 (w), 988 (w), 794 (w), 762 (w).

Caution: *Due to the explosive nature of cyano functional groups, all the experiments were undertaken with great caution and care. Release of the gases (such as HCN) are harmful and potentially lethal at low levels. Experiments should be undertaken with all the necessary equipment and protective shields.*

2. Characterization and computational details

Single crystals suitable for SC-XRD were obtained within a week and the chemical formula was confirmed by elemental analysis and crystal structure analysis. X-ray diffraction data of complexes **1** and **2** were collected by a Rigaku XtalAB PRO MM007DW diffractometer using Cu-Kα radiation (λ = 1.54184 Å) at 120 and 100 K, respectively. The diffraction data were obtained by ω method. The integration and reduction of the data was carried out by the CrystalAlice PRO program. The least square method is used to refine the structure of the compounds, and the non-hydrogen atoms are determined by anisotropic refinement. Finally, the free solvent molecules in the crystal structure were treated with SQUEEZE. The purity of crystalline samples of the two complexes is confirmed by the powder X-ray diffraction (PXRD) patterns measured at room temperature using RigaKu Miniflex600. Variable-temperature Infrared Spectra of the samples were measured at room temperature using pressed KBr pellets using TENSOR 37 FT-IR at room. The calculated patterns were created with Origin software. The UV-Vis absorption spectra were measured using UV-3600 spectrophotometer at room temperature. Thermo-gravimetric analysis (TGA) data were recorded using a TG-DTA analyzer of Nippon Institute of Physics at a heating rate of 10 °C/min between 30 and 800 °C, under a constant flow of nitrogen. Magnetic measurements were performed by Quantum Design SQUID MPMS-3 magnetometer in the 2.0 to 400 K temperature range with an applied field of 1000 Oe. The differential scanning calorimetry (DSC) measurements were carried out under high purity helium, using pure aluminum as the temperature and enthalpy calibration

(the heating and cooling rates were both 10 K/min), using the TA DSC-25 instrument in the United States. Density functional theory (DFT) calculations of complex **1** and **2** were carried out by Gaussian09 package[3] with TPSSh functional[4], which is known to provide reasonable optimized geometries and HS-LS gap for the SCO systems[5]. Optimization of both low-spin and high-spin species was based on the trinuclear fragments extracted from their single-crystal structures. The redefined versions of Ahlrichs basis sets[6], def2-TZVP and def2-SVP, were applied to metal and non-metal elements, respectively. D3 version of Grimme's dispersion correction with Becke-Johnson damping was used in all calculations[7]. Optimized bond lengths around the ls-Fe(II) center are averaged Fe−$N_{cyanide}$ of 1.928 Å, Fe−N_{py} of 1.976 Å and Fe−N_{amine} of 2.022 Å for complex **1**, and averaged Fe−$N_{cyanide}$ of 1.914 Å, Fe−N_{py} of 1.965 Å and Fe−N_{amine} of 2.001 Å for complex **2**, qualitatively consistent with the observations. Calculations of vibrational frequencies were also performed to guarantee the reliability for the optimized geometries, and no imaginary frequencies were found. With a common scaling factor of 0.98, the calculated IR spectra can be compared to the experimental ones. The HS-LS gap (with zero-point energy correction) in case of complex **1** was found to be 8.78 kcal/mol, whereas the value of energy gap in complex **2** is 8.66 kcal/mol with correct signs, falling in a reasonable range for the high-temperature SCO species. The small difference in the energy gap of the two complexes is reasonable due to the similar coordination environments.

Table S1 Trinuclear Iron Complexes

Trinuclear system	Complex Formula	SCO Transition Temperature	SCO center	Reference
Fe^{II}_3	**$[Fe_3(Ettrz)_6(H_2O)_6](CF_3SO_3)_6$** (Ettrz = 4-ethyl-1,2,4-triazole)	205 K	Central Fe^{II} ion	[24]
	$Fe_3(Rtr)_6(H_2O)_6(CF_3SO_3)_6$ (R = alkyl group, tr= 1,2,4-triazole)	≈203 K	Central Fe^{II} ion	[25]
	$[[Fe_3(Settrz)_6(H_2O)_6].5H_2O$ (Settrz= 4-(1,2,4-triazol-4-yl)ethane sulfonate)	$T_{1/2}(\uparrow)$ =357 K, $T_{1/2}(\downarrow)$ =343K	Central Fe^{II} ion	[26]
	$[Fe_3(bntrz)_6(tcnset)_6]$ (bntrz= 4-(Benzyl)-1,2,4-triazole, tcnset= 1,1,3,3-tetracyano-2-thioethylpropenide)	318 K	All three Fe^{II} centres	[27]
	$[Fe_3(p\text{-}MeOptrz)_6(H_2O)_6](tos)_6\cdot 4H_2O$ **$[Fe_3(p\text{-}MeOptrz)_6(H2O)_3]\text{-}(tos)_6$** (p-MeOptrz = 4-(p-Methoxyphenyl)-l,2,4-triazole, tos =Tosylate)	245 K 330 K	Central Fe^{II} ion Central Fe^{II} ion	[28]
	$[Fe_3(iPrtrz)_6(H_2O)_6](Tos)_6\cdot 2H_2O$ **$[Fe_3(iPrtrz)_6(H_2O)_6](CF_3SO_3)_6$** (iptrz = 4-isopropyl-1,2,4-triazole, Tos= p-toluenesulfonate)	242 K 185 K	Central Fe^{II} ion Central Fe^{II} ion	[29]
	$[Fe_3(hyetrz)_6(H_2O)_6](CF_3SO_3)_6$ (hyetrz = 4-(29-hydroxyethyl)-1,2,4-triazole)	290 K	Central Fe^{II} ion	[30]
	$[Fe_3(npt)_6(EtOH)_4(H_2O)_2](ptol)_6\cdot 4EtOH$ (npt= 4-(40-nitrophenyl)-1,2,4-triazole, ptol= p-tolylsulfonate	148 K	Central Fe^{II} ion	[31]
	$[Fe_3(furtrz)_6(ptol)_2(MeOH)_4](ptol)_4\cdot 4(MeOH)$ (furtrz =furanylidene-4H-1,2,4-triazol-4-amine, ptol = p-tolylsulfonate)	≈170 K	Central Fe^{II} ion	[32]
	$[Fe_3(NH_2\text{-}trz)_6(SCN)_4(H_2O)_2](SCN)_2\cdot H_2O$ **$[Fe_3(NH_2\text{-}trz)_6(SCN)_5(H_2O)](SCN)$** ($NH_2$-trz = 4-amino-1,2,4-triazole)	202 K 160 K	Central Fe^{II} ion Central Fe^{II} ion	[33]
	$[Fe_3(PyTrz)_8(H_2O)_4](NO_3)_6)$ 4-(2-pyridyl)-1,2,4-triazole (PyTrz)	208 K	Central Fe^{II} ion	[34]
	$[Fe_3(Prtrz)_6(ReO_4)4(H_2O)_2](ReO_4)2\cdot H_2O$ (L=4-propyl-1,2,4-triazole)	185 K	Central Fe^{II} ion	[35]
	$[Fe_3(\mu\text{-}L)_6(H_2O)6]^{6-}$ [L = 4-(1,2,4-triazol-4-yl)ethanedisulfonate)]	$T_{1/2}(\uparrow)$ = 400 K, $T_{1/2}(\downarrow)$ = 310 K	Central Fe^{II} ion	[36]
	$[Fe_3L_2(NCS)_4(H_2O)]$ (L=1,3-bis[(2-pyridylmethyl)imino]propan-2-ol	120–240 K	Central Fe^{II} ion	[37]
$Fe^{III}_2Fe^{II}$	**$[Fe^{III}_2Fe^{II}(CN)_6(tp^*)_2(tpa)]\cdot 4MeCN\cdot t\text{-}BuMeO$** (tp* = hydrotris(dimethylpyrazolyl)borate, bpym = 2,2'-bipyrimidine)	340 K	Central Fe^{II} ion	[19]
	$\{[Tp^*Fe^{III}(CN)_3]_2Fe^{II}(Bpi)_4\}\cdot 2H_2O$ **$\{[Tp^{Me}Fe^{III}(CN)_3]_2Fe^{II}(Bpi)_4\}\cdot 4H_2O$** **$\{[TpFe^{III}(CN)_3]_2Fe^{II}(Bpi)_4\}\cdot 4H_2O$** (Bpi= 1-biphenyl-4-yl-1Himidazole, Tp^*=hydridotris (3,5-dimethylpyrazol-1-yl)borate, Tp^{Me}=hydridotris(3-methylpyrazol-1-yl)borate, Tp=hydrotris(pyrazolyl) borate)	182 K 200 K 263 K	Central Fe^{II} ion Central Fe^{II} ion Central Fe^{II} ion	[38]
	$[Fe^{II}Fe^{III}_2(HATD)_4(H_2O)_4]\cdot 4DMA\cdot 3H_2O$, **$[Fe^{II}Fe^{III}_2(HATD)_4(DMF)_2(H_2O)_2]\cdot 2DMF\cdot 2H_2O$** (DMA = N,N-dimethylacetamide, DMF = N,N-dimethylformamide, HATD=azotetrazolyl-2,7-dihydroxynaphthalene)	High temperature SCO	Terminal Fe^{III} centres	[39]
	$\{[Fe^{II}(TPMA)][Fe^{III}(Tp^*)(CN)_3]_2\}.MeOH.2H_2O$, **$\{[Fe^{II}(TPMA)][Fe^{III}(Tp)(CN)_3]_2\}\cdot H_2O$**	$T_{1/2}$ =410 K (fresh sample), $T_{1/2}$ =406 K (dried sample) $T_{1/2}$ =283 K (fresh sample); $T_{1/2}(\uparrow)$ =283 K, $T_{1/2}(\downarrow)$ = 257 K (dried sample)	Central Fe^{II} ion Central Fe^{II} ion	This work

Table S2 Main crystallographic parameters of complex **1** and **2**.

Compound reference	**1**	**2**
Chemical Formula	$C_{54}H_{62}B_2Fe_3N_{22}$	$C_{42}H_{38}B_2Fe_3N_{22}$
Formula Mass	1208.42	1040.1
Temperature/K	120	100
Crystal system	triclinic	monoclinic
Space group	*P*-1	$P2_1/c$
***a*/Å**	15.1055(4)	14.1399(2)
***b*/Å**	15.2765(5)	13.4080(2)
***c*/Å**	17.9517(5)	27.1794(4)
***α*/°**	66.834(3)	90
***β*/°**	84.748(2)	101.147(1)
***γ*/°**	63.152(3)	90
***V*/Å^3**	3379.2(2)	5055.6(7)
Z	2	4
***μ*/mm^{-1}**	5.492	7.279
***F*(000)**	1256	2168
Radiation type	CuKα	CuKα
Reflections collected	34602	27440
Θ range (deg)	5.384−146.908	7.38-152.706
R_{int}	0.0329	0.0474
R_1 ($I > 2\sigma(I)$)[a]	0.0422	0.0793
$wR(F^2)$ ($I > 2\sigma(I)$)[b]	0.1152	0.2058
R_1 (all data)[a]	0.0470	0.0869
$wR(F^2)$ (all data)[b]	0.1182	0.2099
GOF	1.087	1.062
CCDC number	2105094	2105095

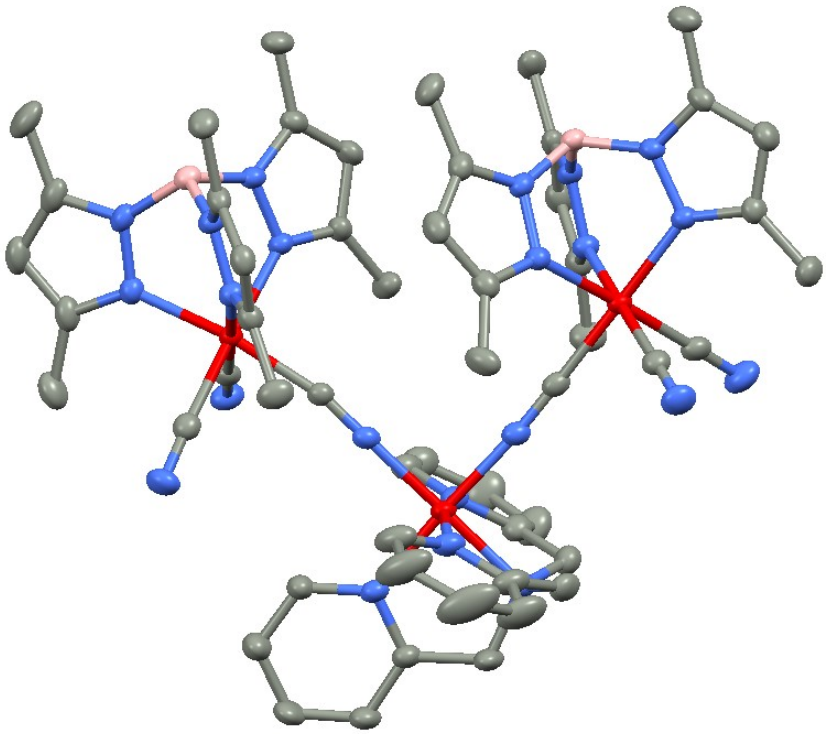

(a) complex **1**

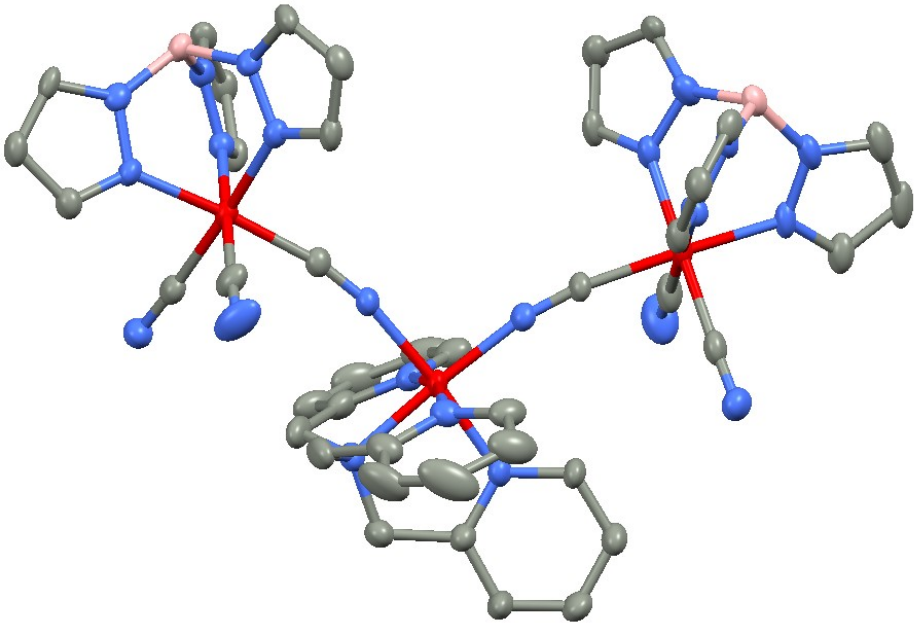

(b) complex **2**

Fig. S1 Thermal ellipsoid structure (50%) of complex (a) **1** and (b) **2**.

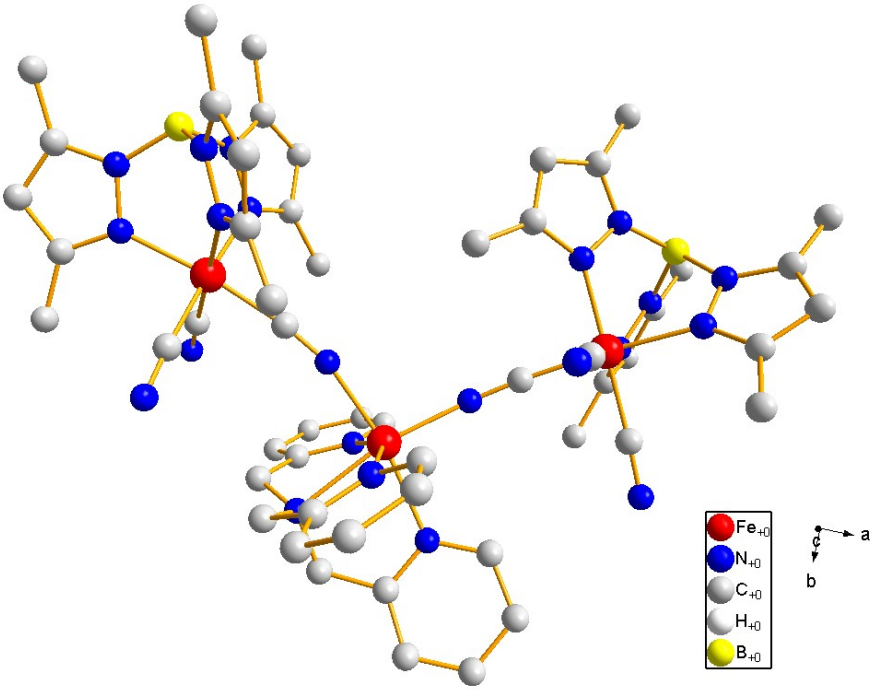

Fig. S2 Simulated high spin (HS) structure of complex **1**.

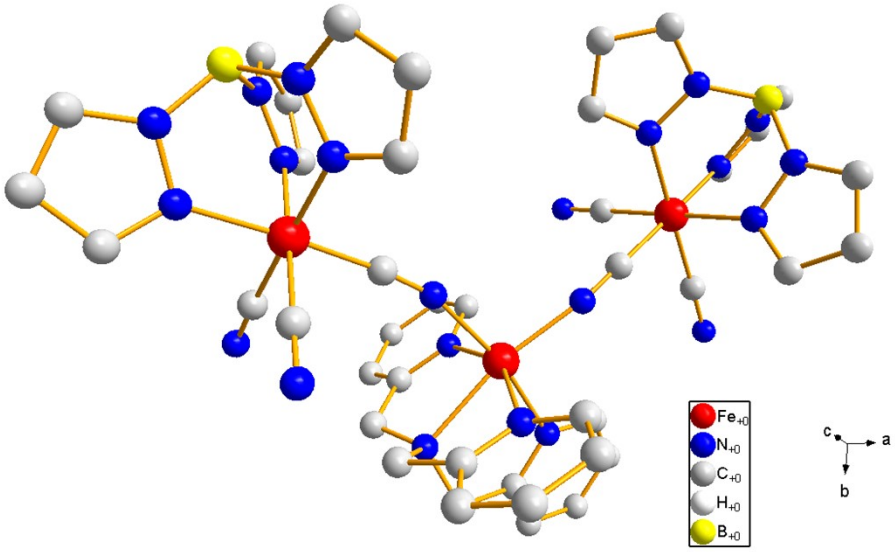

Fig. S3 Simulated high spin (HS) structure of complex **2**.

Table S3 Selected bond distances of LS (experimental) and HS (simulated) states of complex **1** and **2**.

	1 (Exp. LS)	**1** (Sim. HS)	**2** (Exp. LS)	**2** (Sim. HS)
Fe3−N1	1.9505(19)	2.052(5)	1.968(1)	2.044
Fe3−N10	1.9588(19)	2.248(5)	1.976(2)	2.224
Fe3−N11	1.9699(19)	2.182(5)	2.012(5)	2.174
Fe3−N12	1.9935(19)	2.322(4)	1.984(2)	2.283
Fe3−N13	1.962(2)	2.191(5)	1.950(7)	2.175
Fe3−N14	1.9378(19)	2.090(5)	1.976(3)	2.075
Fe3−N(Average)	1.9621(16)	2.181(5)	1.977(6)	2.162(5)
Fe3···Fe1	5.002(3)	5.095(4)	4.988(9)	5.058(8)
Fe3···Fe2	5.005(4)	5.045(3)	4.985(3)	5.013(1)
Fe1···Fe2	7.100(3)	8.459(3)	8.301(8)	8.439(6)
Fe1−C1−N1	165.99(19)	172.40(4)	168.85(3)	175.65(9)
Fe2−C37−N16	175.5(2)	173.95(3)	168.46(2)	174.35(1)
Fe3−N1−C1	177.53(18)	165.57(3)	169.21(5)	160.64(6)
Fe3−N16−C37	175.62(18)	163.09(4)	170.16(3)	163.23(5)
Fe1···Fe3···Fe2	90.38(19)	113.07(3)	112.68(5)	113.84(5)

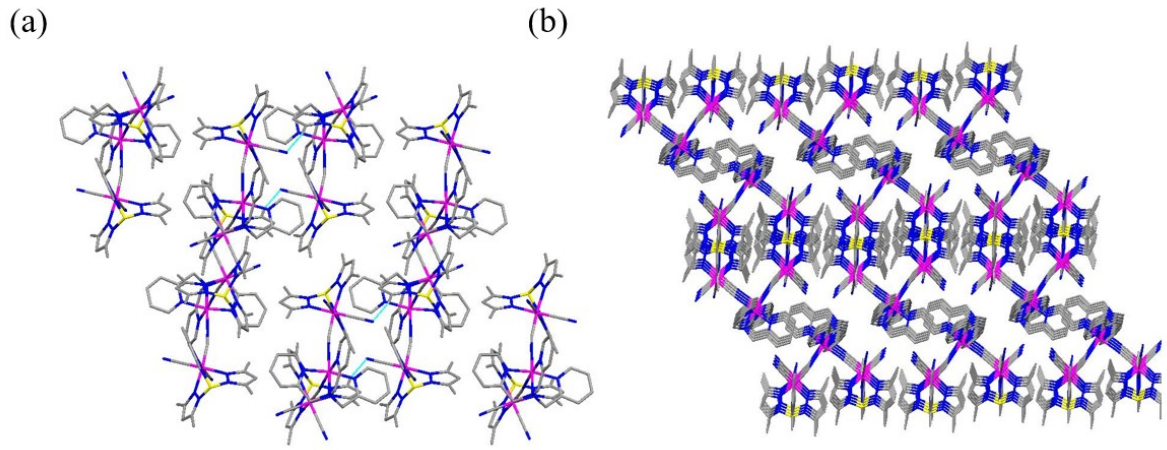

Fig. S4 (a) The 2D packing structure of complex **1** extended along the *ab* plane formed by hydrogen bonding. (b) The 3D stacking structure of complex **1** (hydrogen atoms and solvent molecules are omitted for clarity).

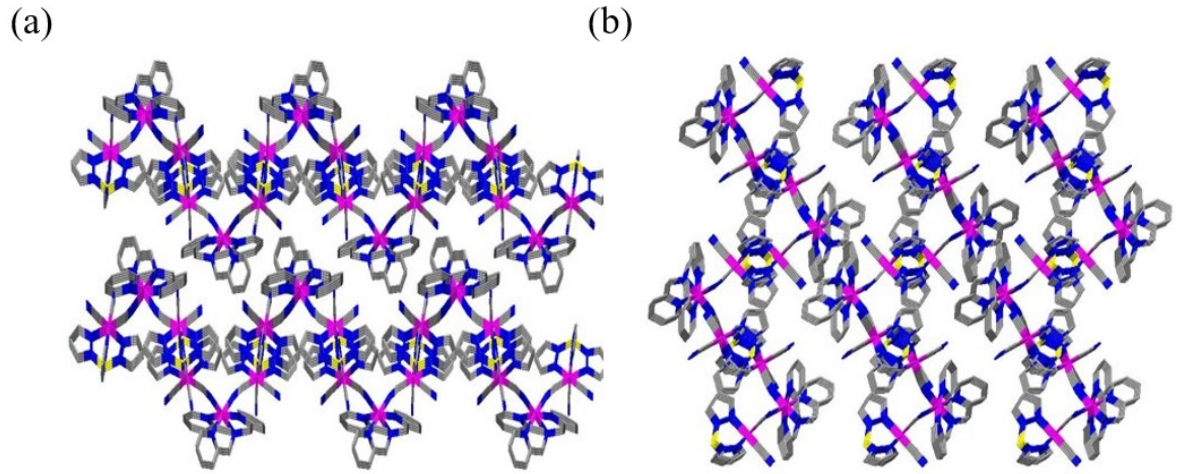

Fig. S5 (a) The 2D packing structure of complex **2** extended along the *ac* plane. (b) The 3D packing structure of complex **2** (hydrogen atoms and solvent molecules are omitted for clarity).

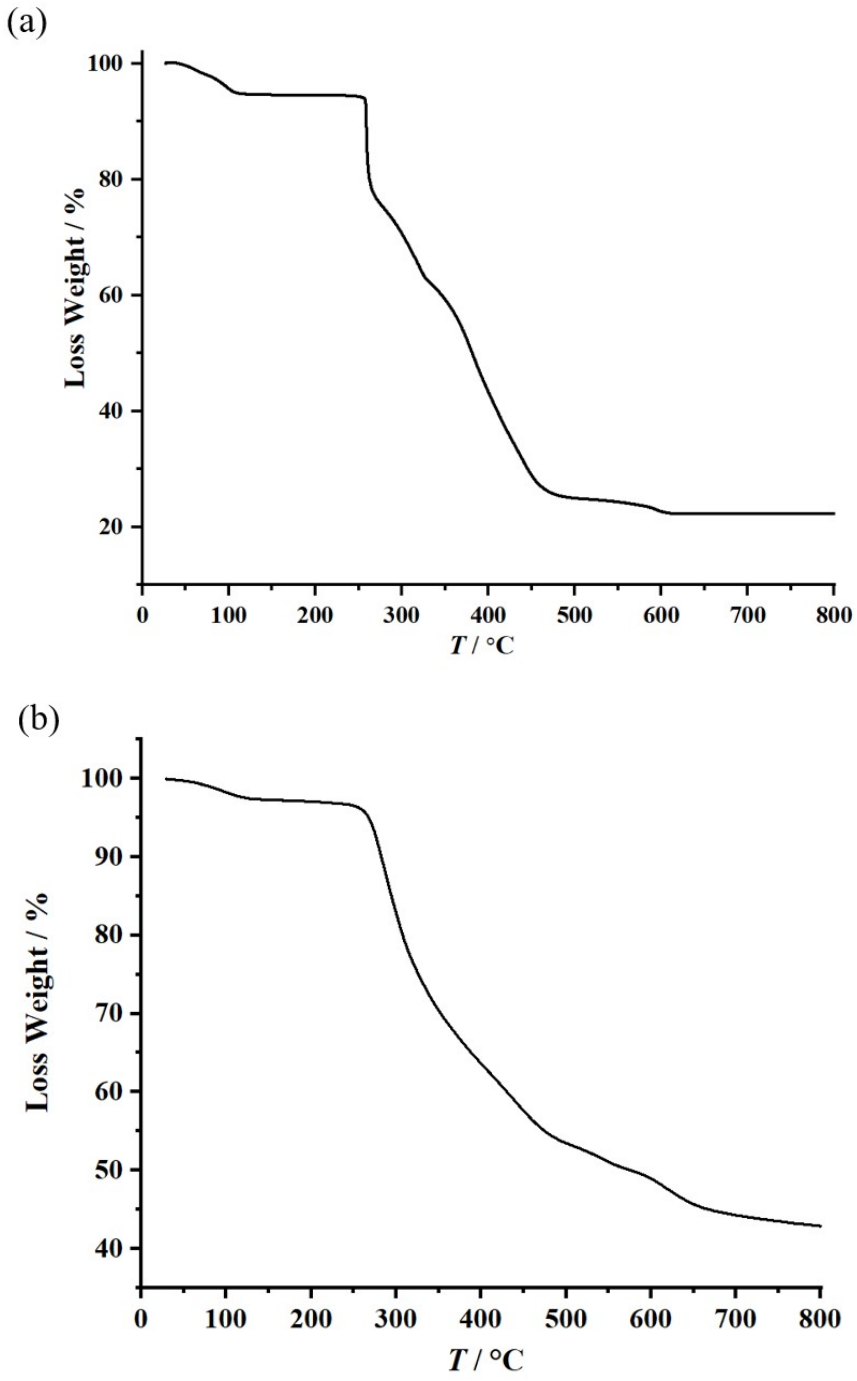

Fig. S6 TGA plots of complex **1** (a) and **2** (b) from 30°C to 800°C (heating rate: 10 °C/min).

Table S4 Unit cell parameters of the fresh and dried sample of complex **2** at 100 K.

Complex 2	**Fresh sample**	**Dried sample**
Temperature/K	100	100
Crystal system	monoclinic	monoclinic
Space group	$P2_1/c$	$P2_1/c$
***a*/Å**	14.1399(2)	13.1336(3)
***b*/Å**	13.4080(2)	14.1116(6)
***c*/Å**	27.1794(4)	26.3026(13)
***α*/°**	90	90
***β*/°**	101.147(1)	90.637(3)
***γ*/°**	90	90
***V*/Å^3**	5055.6(7)	4874.5(3)

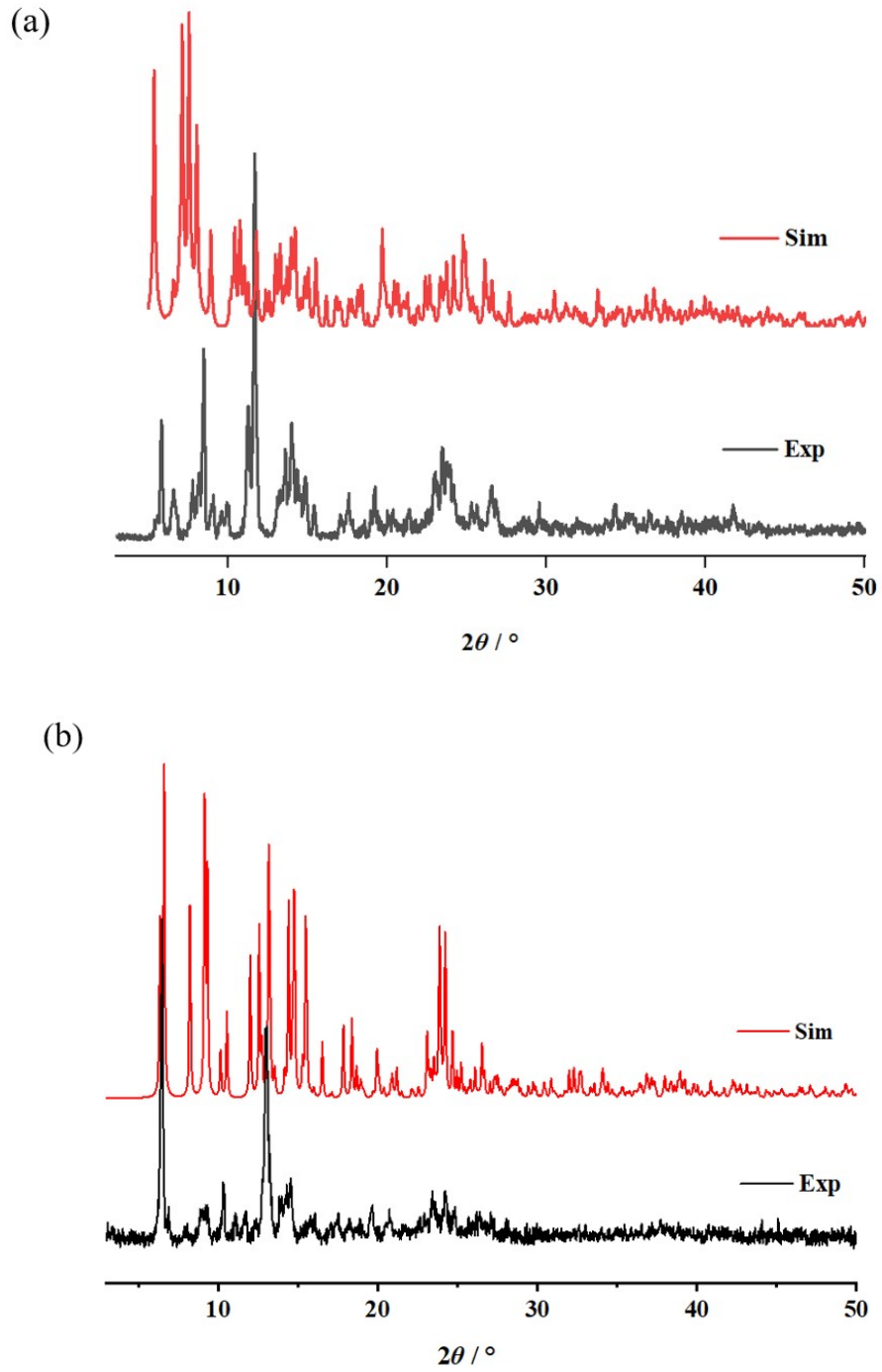

Fig. S7 PXRD profiles of complex (a) **1** and (b) **2**: simulation results (Sim) and experimental results (Exp).

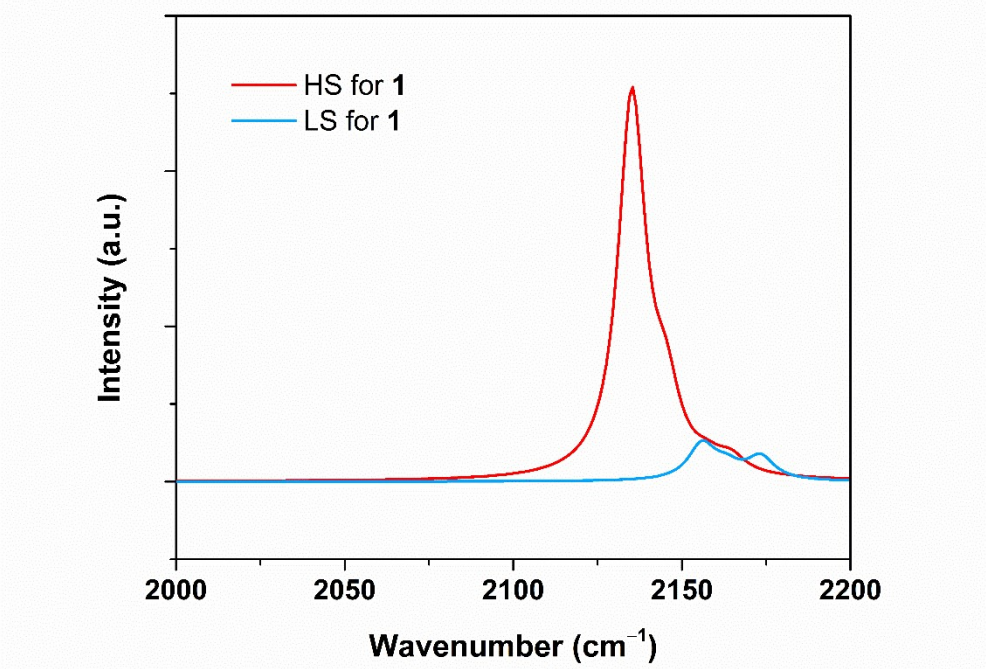

(a) complex **1**

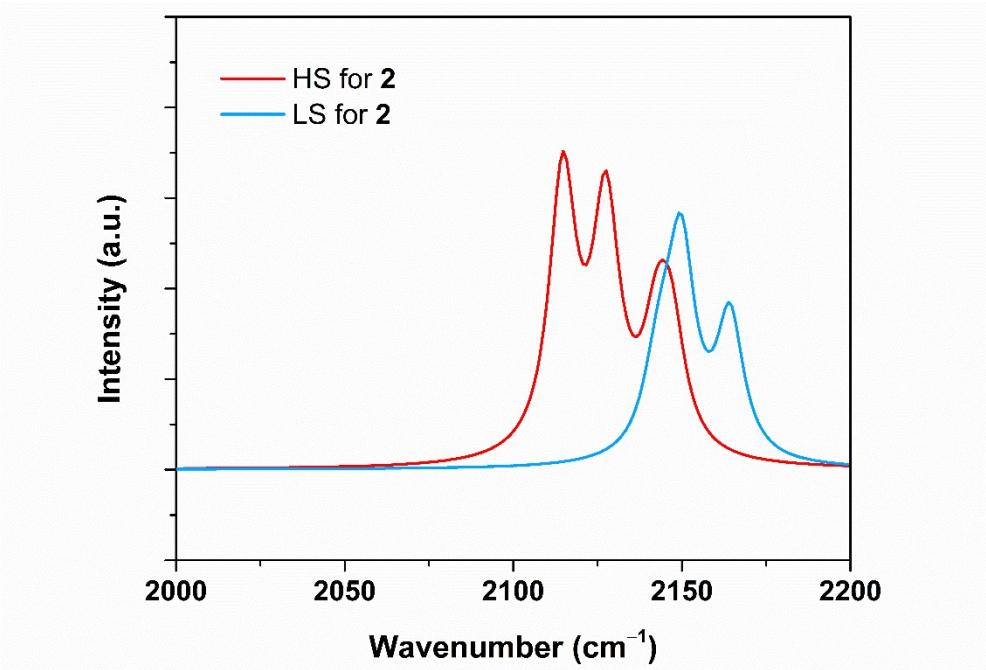

(b) complex **2**

Fig. S8 Calculated IR spectra (highlighting the CN stretching frequencies) of complex (a) **1** and (b) **2**, which are consistent with the exponential ones.

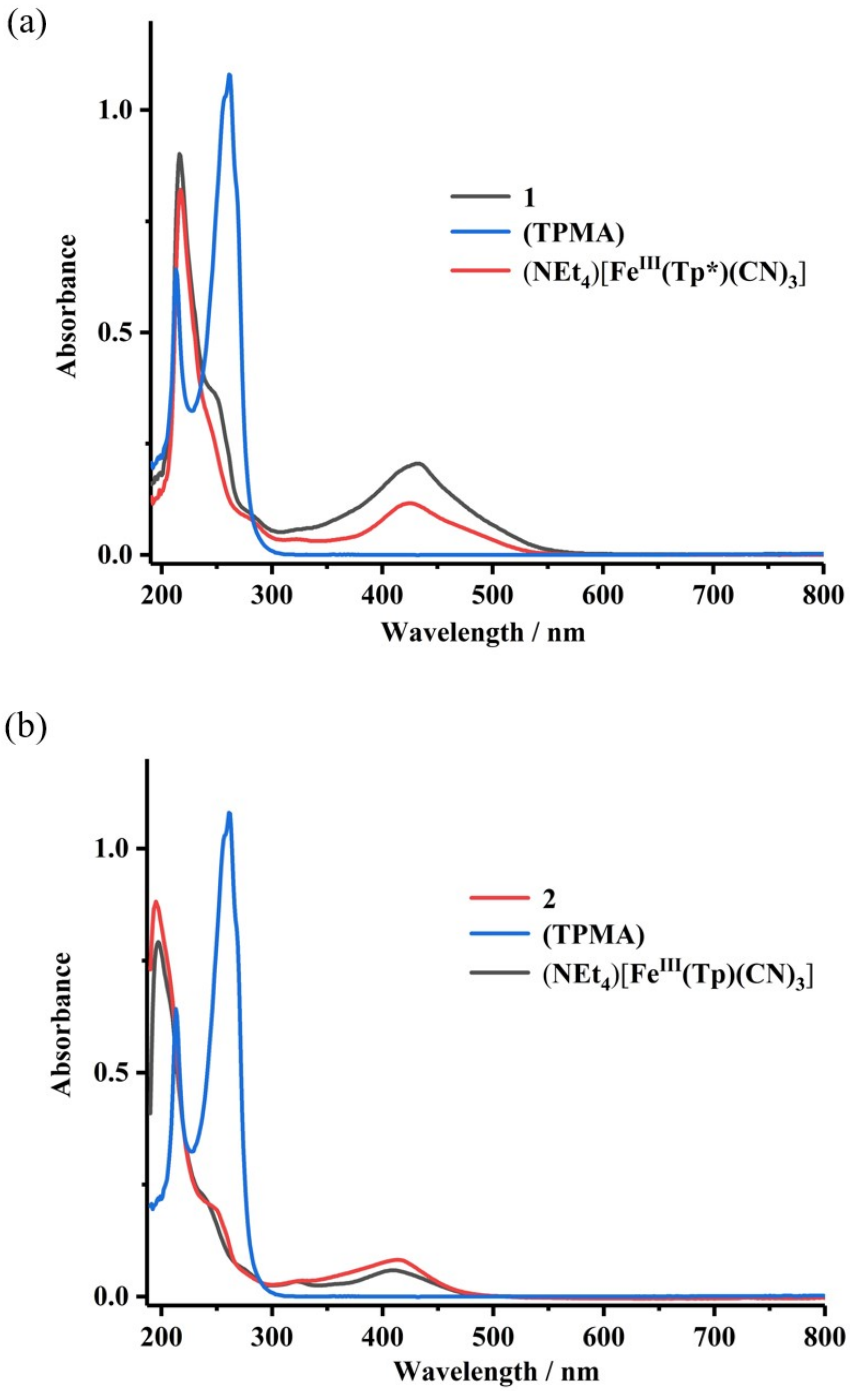

Fig. S9 (a) UV-Vis absorption spectra of ligand TPMA, intermediate $[NEt_4][Fe^{III}(Tp^*)(CN)_3]$ and complex **1** in acetonitrile solution at room temperature. (b) UV-Vis absorption spectra of ligand TPMA, intermediate $[NEt_4][Fe^{III}(Tp)(CN)_3]$ and complex **2** in acetonitrile solution at room temperature.

References

[1] T. Kojima, R. A. Leising, S. Yan, L. Que, Jr., *J. Am. Chem. Soc.* **1993**, *115*, 11328-11335.

[2] (a) D. Li, S. Parkin, G. Wang, G. T. Yee, A. V. Prosvirin and S. M. Holmes, Inorg. Chem. **2005**, *44,* 4903-4905; (b) M. Nihei, Y. Sekine, N. Suganami, K. Nakazawa, A. Nakao, H. Nakao, Y. Murakami and H. Oshio, J Am Chem Soc **2011**, *133,* 3592-3600.

[3] Gaussian 09, Revision D.01, M. J. Frisch, G. W. Trucks, H. B. Schlegel, G. E. Scuseria, M. A. Robb, J. R. Cheeseman, G. Scalmani, V. Barone, B. Mennucci, G. A. Petersson, H. Nakatsuji, M. Caricato, X. Li, H. P. Hratchian, A. F. Izmaylov, J. Bloino, G. Zheng, J. L. Sonnenberg, M. Hada, M. Ehara, K. Toyota, R. Fukuda, J. Hasegawa, M. Ishida, T. Nakajima, Y. Honda, O. Kitao, H. Nakai, T. Vreven, J. A. Montgomery, Jr., J. E. Peralta, F. Ogliaro, M. Bearpark, J. J. Heyd, E. Brothers, K. N. Kudin, V. N. Staroverov, T. Keith, R. Kobayashi, J. Normand, K. Raghavachari, A. Rendell, J. C. Burant, S. S. Iyengar, J. Tomasi, M. Cossi, N. Rega, J. M. Millam, M. Klene, J. E. Knox, J. B. Cross, V. Bakken, C. Adamo, J. Jaramillo, R. Gomperts, R. E. Stratmann, O. Yazyev, A. J. Austin, R. Cammi, C. Pomelli, J. W. Ochterski, R. L. Martin, K. Morokuma, V. G. Zakrzewski, G. A. Voth, P. Salvador, J. J. Dannenberg, S. Dapprich, A. D. Daniels, O. Farkas, J. B. Foresman, J. V. Ortiz, J. Cioslowski, and D. J. Fox, Gaussian, Inc., Wallingford CT, **2013**.

[4] (a) J. M. Tao, J. P. Perdew, V. N. Staroverov, and G. E. Scuseria, *Phys. Rev. Lett.*, **91** (2003) 146401. (b) V. N. Staroverov, G. E. Scuseria, J. Tao and J. P. Perdew, *J. Chem. Phys.*, 2003, **119**, 12129.

[5] J. Cirera, M. Via-Nadal, and E. Ruiz, *Inorg. Chem.* **2018**, 57, 22, 14097–14105.

[6] (a) A. Schaefer, H. Horn, and R. Ahlrichs, *J. Chem. Phys.*, **97** (1992) 2571-77. (b) F. Weigend and R. Ahlrichs, *Phys. Chem. Chem. Phys.*, **7** (2005) 3297-305.

[7] S. Grimme, J. Antony, S. Ehrlich and H. Krieg, *J. Chem. Phys.*, **132** (2010) 154104.